

Nonradiative dynamics determined by charge transfer induced hydrogen bonding: A combined femtosecond time-resolved fluorescence and density functional theoretical study of methyl dimethylaminobenzoate in water

Chensheng Ma,^a Yue-qun Ou,^a Chris Tsz-Leung Chan,^a Allen Ka-Wa Wong,^b Ruth Chau-Ting Chan,^b Bowie Po Yee Chung,^b Chao Jiang,^a Ming-Liang Wang,^{a*} Wai-Ming Kwok^{b*}

^aCollege of Chemistry and Environmental Engineering, Shenzhen University, Shenzhen, Guangdong, P. R. China.

^b Department of Applied Biology and Chemical Technology, The Hong Kong Polytechnic University, Hung Hom, Kowloon, Hong Kong, P. R. China.

E-mail: wangml@szu.edu.cn, wm.kwok@polyu.edu.hk

Method of fluorescence quantum yield measurement..	2
Equation of log-normal line shape function.....	2
Table S1 Spectral parameters from log-normal simulation of fs-TRF of MDMABA in 70%H ₂ O/30%CH ₃ CN	2
Figure S1 Example for deconvolution using log-normal simulation of fs-TRF spectrum	2
Method of kinetic analysis for fs-TRF intensity decay ..	3
Figure S2 Fs-TRF spectra of MDMABA in 70%D ₂ O/30% CH ₃ CN	3
Figure S3 Frontier orbital calculated for MDMABA-S(H ₂ O) in S ₀ , LE, and ICT state.....	3
Figure S4 Frontier orbital calculated for MDMABA-2H ₂ O-S in S ₀ , LE, and ICT state..	3
Figure S5 Potential energy curve along the twisting angle of free MDMABA in S ₀ and S ₁ state..	3
Table S2 Fs-TRF kinetic parameters of MDMABA in 70%H ₂ O/30%CH ₃ CN and 70%D ₂ O/30%CH ₃ CN.....	4
Table S3 Details of optimized structural parameters and total energies calculated for S ₀ , LE, and ICT state of MDMABA in the varied forms .	4
Table S4 H-binding energies calculated for MDMABA-2H ₂ O complex in the S ₀ , LE, and ICT state.....	5

Measurement of fluorescence quantum yield

The fluorescence quantum yields of the sample solution ($\Phi_{f(X)}$) were calculated according to the following equation:

$$\Phi_{f(X)} = \frac{F_X}{F_S} \times \frac{A_S}{A_X} \times \left(\frac{n_X}{n_S}\right)^2 \times \Phi_{f(S)}$$

Where,

F_X : integrated intensity of the acquired fluorescence spectrum for the sample

F_S : integrated intensity of the acquired fluorescence spectrum for the standard

A_X : absorbance of the sample at the excitation wavelength

A_S : absorbance of the standard at the excitation wavelength

n_X : refractive index of the solvent used for the sample

n_S : refractive index of the solvent used for the standard

$\Phi_{f(S)}$: fluorescence quantum yield of the standard

Equation of log-normal line shape function

$$F(v) = h \begin{cases} \exp[-\ln(2)\{\ln(1+\alpha)/\gamma\}^2] & \alpha > -1 \\ 0 & \alpha \leq -1 \end{cases} \dots \dots \dots \text{(eq.1)}$$

$$\alpha \equiv 2\gamma(v-v_p)/\Delta$$

Where,

h : the peak intensity of the spectrum

v_p : the maximum frequency of the spectrum

γ : asymmetry parameter of the spectrum

Δ : width parameter of the spectrum

The above four parameters were adjusted in the nonlinear least-square fitting to simulate the spectral profile of the experimental steady state and fs-TRF spectra. To perform the spectral simulation, we have firstly represented the spectra in the unit of wavenumber (v , cm^{-1}) by using the relation $F(v) = \lambda^2 F(\lambda)$.

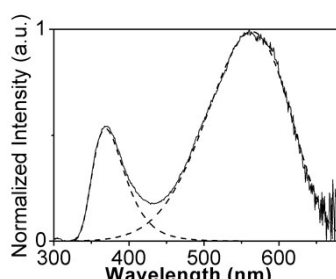
The log-normal simulation can also produce the integrated intensity (I) of the spectra as expressed in the following equation:

$$I = [\pi/4\ln(2)]^{1/2} h \Delta \exp[\gamma^2/4\ln(2)] \dots \dots \dots \text{(eq. 2)}$$

Table S1 Band width (Δ) and maximum frequency (v_p) obtained by log-normal simulation of the ICT spectra at the varied delay times after photo-excitation of MDMABA in 70% $\text{H}_2\text{O}/30\% \text{CH}_3\text{CN}$

Delay time	3 ps	3.5 ps	4 ps	5 ps	6 ps
$\Delta (\text{cm}^{-1})$	5832.430	4846.418	4467.319	4143.661	3919.863
$v_p (\text{cm}^{-1})$	18163.136	17911.752	17809.003	17733.647	17711.622

Fig S1 Deconvolution by log-normal function of the 5 ps fs-TRF spectrum from MDMABA in 70% $\text{H}_2\text{O}/30\% \text{CH}_3\text{CN}$. The spectrum in solid is the experimental data, those in the dash lines are the simulated spectrum for the LE and ICT fluorescence, respectively



Kinetic analysis of the fs-TRF intensity decay:

For the analysis of kinetic decays of the fs-TRF intensities, the experimental time profiles ($F(t)$) were fitted by convolution of the instrument response function ($g(t)$) with a multiple exponential function ($f(t)$) as showed in the following equations (eq. 3-5):

Where τ_i is the time constant and a_i the corresponding amplitude associated to the τ_i of the TRF intensity decay. For the current case, a three-exponential function with $n = 3$ was used for $f(t)$ in fitting the experimental fs-TRF intensity decays

Fig. S2 Temporal evolution of fs time-resolved fluorescence spectra recorded at (a) 0.5-100 ps and (b) 6-400 ps after 300 nm excitation of MDMABA in 70% D_2O /30% CH_3CN . The arrows indicate direction of temporal evolution of the TRF spectra. Inset in (a) shows change with time the spectral profile of ICT fluorescence at \sim 3 to 6 ps after the photo-excitation

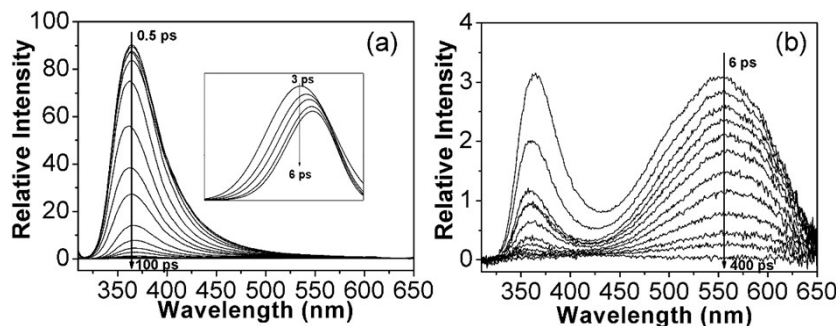


Fig. S3 Diagram of the HOMO and LUMO calculated for MDMABA-S (H_2O) in the S_0 , LE, and ICT states.

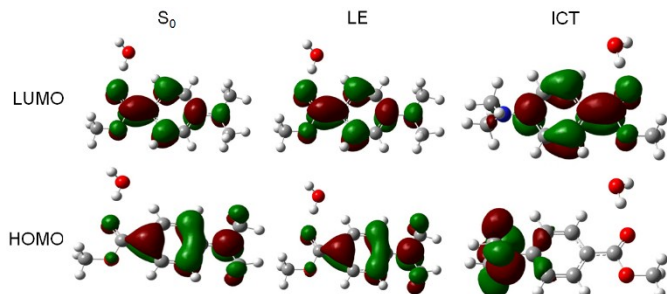


Fig. S4 Diagrams of the HOMO and LUMO calculated for MDMABA- $2\text{H}_2\text{O-S}$ in the S_0 , LE, and ICT state

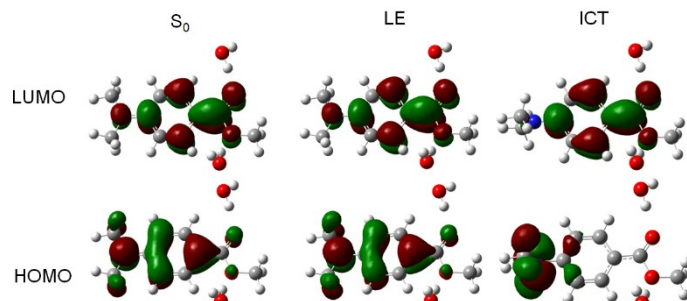


Fig. S5 Variation of potential energy as a function of the twisting angle (C4-C5-N11-C16) of MDMABA in the S_0 and lowest energy excited singlet (S_1) state

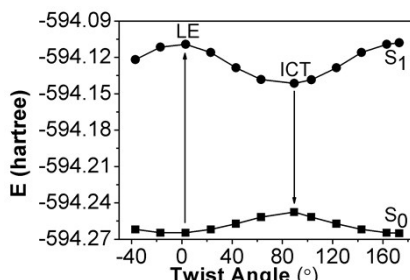


Table S2 Time constant ($\tau_{i=1,2,3}$) and the corresponding relative contribution ($a_{i=1,2,3}$) obtained from kinetic analysis of the fs-TRF intensity decays the different emission wavelengths from MDMABA in 70%H₂O/30%CH₃CN and 70%D₂O/30%CH₃CN

	70%H ₂ O/30%CH ₃ CN			70%D ₂ O/30%CH ₃ CN		
	τ_1/a_1	τ_2/a_2	τ_3/a_3	τ_1/a_1	τ_2/a_2	τ_3/a_3
	0.7 ps	2.1 ps	49.7 ps	0.7 ps	2.6 ps	76.6 ps
360 nm	0.97	0.28	0.00	0.97	0.31	0.07
560 nm	0.03	0.41	0.40	0.03	0.39	0.35
590 nm	0.00	0.31	0.60	0.00	0.31	0.58

Table S3 Main optimized structural parameters of the bond lengths (in Å), bond angles (in degree), dihedral angles (in degree) and the total energy (in hartree) in the S₀, LE, and ICT state for MDMABA in the varied examined forms

	MDMABA			MDMABA-S			MDMABA-H ₂ O-S			MDMABA-2H ₂ O-S			
	S ₀	LE	ICT	S ₀	LE	ICT	S ₀	LE	ICT	S ₀	LE	ICT	
C1-C2	1.401	1.418	1.433	1.405	1.432	1.438	1.406	1.430	1.437	1.407	1.427	1.437	
C2-C3	1.401	1.433	1.433	1.404	1.432	1.437	1.405	1.430	1.436	1.406	1.428	1.437	
C3-C4	1.384	1.394	1.373	1.382	1.381	1.374	1.381	1.382	1.375	1.380	1.383	1.375	
C4-C5	1.416	1.410	1.416	1.421	1.423	1.416	1.422	1.422	1.414	1.422	1.421	1.413	
C5-C6	1.416	1.433	1.414	1.421	1.425	1.416	1.422	1.423	1.414	1.422	1.421	1.411	
C6-C1	1.385	1.378	1.376	1.383	1.380	1.376	1.382	1.382	1.376	1.381	1.383	1.376	
C5-N11	1.379	1.410	1.444	1.367	1.397	1.429	1.365	1.397	1.430	1.364	1.398	1.431	
N11-C12	1.455	1.446	1.440	1.459	1.449	1.445	1.460	1.449	1.445	1.460	1.450	1.445	
N11-C16	1.455	1.449	1.440	1.459	1.450	1.445	1.460	1.450	1.445	1.460	1.450	1.445	
C20-021	1.213	1.232	1.234	1.221	1.252	1.248	1.227	1.258	1.258	1.224	1.256	1.255	
C20-O22	1.358	1.379	1.391	1.352	1.384	1.391	1.346	1.376	1.383	1.357	1.386	1.398	
C2-C20	1.477	1.460	1.436	1.472	1.449	1.426	1.467	1.450	1.422	1.464	1.451	1.420	
O21-H29							1.845	1.770	1.745	1.859	1.784	1.756	
O22-H31										2.032	1.959	1.911	
O21-C20-O22	122.33	122.74	120.99	122.08	121.88	120.10	121.33	121.13	119.50	120.81	121.09	118.94	
O21-C20-C2	125.06	124.33	126.27	124.99	125.25	126.56	125.34	125.65	126.56	125.69	125.31	127.21	
O22-C20-C2	112.60	112.91	112.74	112.93	112.88	113.34	113.33	113.23	113.94	113.50	113.58	113.84	
C16-N11-C12	118.57	118.00	120.98	119.21	118.96	121.14	119.16	119.00	121.24	119.11	118.99	121.29	
C4-C5-N11-C12	6.86	6.86	-89.52	0.060	0.092	-89.89	-0.22	-0.22	-90.28	0.71	0.71	90.18	
C4-C5-N11-C16	173.03	173.03	89.40	179.92	179.94	89.82	179.75	-179.75	89.75	179.26	179.26	-89.84	
C6-C5-N11-C16	-7.211	13.796	-90.48	-0.085	-0.074	-90.16	0.26	0.38	-90.35	-0.670	-1.35	90.36	
C3-C2-C20-O21	0.120	-0.670	0.003	0.010	0.006	-0.00	0.76	0.42	0.73	-8.64	-4.84	-4.56	
C3-C2-C20-O22	-179.89	177.81	180.00	180.00	-179.99	180.00	179.22	-179.51	-178.73	171.17	173.96	174.34	
C1-C2-C20-O21	180.00	179.72	180.00	180.00	-180.00	180.00	179.24	-179.56	-179.46	170.53	174.87	175.29	
C1-C2-C20-O22	-0.22	-1.232	-0.004	0.006	0.00	0.00	0.79	0.51	1.08	-9.66	-6.33	-5.81	
C2-C20-O22-C23	-180.00	179.90	-	180.00	180.00	180.00	179.88	-179.87	-179.40	175.27	170.99	170.34	
O21-C20-O22-C23	0.02	-1.59	0.00	0.00	-0.01	0.00	0.14	0.19	1.10	-4.91	-10.15	-10.66	
E	-594.27	-	594.11	594.14	594.27	-594.14	594.16	670.75	-670.61	-670.63	747.22	-747.08	747.11

Table S4 Calculated stabilization energies (E_H) of the H-bonding involved in the hydrogen-bonded complex MDMABA-2H₂O in the S_0 , LE, and ICT state. $E_{H(C=O)}$ and $E_{H(C-O)}$ are the stabilization energy due to the C20=O21···H29-O27 and C20-O2···H31-O30 H-bonding, respectively.

	E_H (kcal/mol)	$E_{H(C=O)}$ (kcal/mol)	$E_{H(C-O)}$ (kcal/mol)
S_0	8.54	5.68	2.86
LE	12.08	7.90	4.17
ICT	13.55	8.61	4.94